Electrochemical, Electron Spin Resonance and Nuclear Magnetic Resonance Investigations of Tertiary Phosphine Complexes of Nickel. Part 1. Mono- and Di-nuclear Nickel Dithiolene and Nickel Dihalide Species†

Graham A. Bowmaker* and Julian P. Williams
Department of Chemistry, University of Auckland, Private Bag 92019, Auckland, New Zealand

The synthesis, characterisation and ^{31}P NMR parameters of $[Ni\{S_2C_2(CN)_2\}(PR_3)_2]$ (PR_3 = $PMePh_2$ or PBu^nPh_2) and of $[\{Ni(S_2C_2R_2)(L\text{–}L)\}_n]$ complexes (L–L = ditertiary phosphine containing vinylene or *ortho*-phenylene interphosphorus linkages, n = 1 or 2, R = CN or Ph) are reported. The ^{31}P NMR data for the $[\{Ni(S_2C_2R_2)(L\text{–}L)\}_n]$ complexes show that the ring contribution to the chemical shift is large and positive for the mononuclear species (n = 1) and near zero or negative for the dinuclear species (n = 2). Electrochemical studies of the complexes and ESR studies of their electrogenerated products have shown variations in electrochemical and ESR parameters due to variations in (*i*) co-ordination ring size, (*ii*) interphosphorus linkage and (*iii*) substituent at phosphorus. The ESR spectrum of the redox product identified as $[Ni\{S_2C_2(CN)_2\}\{C_6H_4(PMePh)(PPh_2)\text{-}1,2\}]^+$ exhibited two chemically inequivalent ^{31}P nuclei. The dinuclear complexes (n = 2) exhibited multiple redox processes. The ESR spectra show that the reduction products involve metal-based electron addition to yield the corresponding nickel(I) species, while the oxidation products involve removal of a primarily ligand-based electron. The one-electron reduction product of the complex $[Ni(S_2C_2Ph_2)\{C_6H_4(PMePh)_2\text{-}1,2\}]$ shows a spectrum characteristic of a nickel(I) monomer ($S = \frac{1}{2}$) at *ca.* 298 K, but is ESR inactive at *ca.* 90 K. This is attributed to the reversible formation of a diamagnetic dimer (S = 0) upon freezing. The reduction products of the complexes $[\{NiX_2(trans\text{-}Ph_2PCH{=}CHPPh_2)\}_2]$ (X = Cl, Br, I or SCN) exhibit no solution ESR spectra at *ca.* 298 K, but for X = I a triplet state (S = 1) spectrum at *ca.* 90 K is observed, characteristic of a dinuclear Ni^I–Ni^I species.

The SEESR (simultaneous electrochemical and ESR) technique is a valuable method for the characterisation of species involved in electrochemical redox processes.[1–3] Metal- and ligand-based redox processes have been determined on the basis of the ESR spectra of electrogenerated products in a SEESR study of metallooctaethylporphyrins.[4] A SEESR study of the effect of variations in the type, degree of unsaturation, charge and ring size of the ligand on the redox behaviour of macrocyclic complexes of nickel has been reported.[5] An investigation of the one-electron reduction processes of the complexes $[Ni(S_2CNR_2)_x(dppe)_{2-x}]^{(2-x)+}$ [x = 0, 1 or 2; R = Et, Bu^n, C_6H_{11} or CH_2Ph; dppe = bis(diphenylphosphino)ethane, $Ph_2PCH_2CH_2PPh_2$], has been reported.[6] The ESR spectrum of the electrogenerated one-electron reduction product of $[Ni(S_2CNBu^n)_2]$ showed line patterns assignable to the expected bis(bidentate) nickel(I) species as well as to a nickel(I) species with an 'unhinged' ligand.[6] In a SEESR study, the complex $[Ni(S_2C_2Ph_2)_2]$ was observed to undergo two reversible one-electron reductions, and one quasi-reversible oxidation process.[7] The unpaired electron in the $[Ni(S_2C_2Ph_2)_2]^-$ complex is assigned as ligand-based from the ESR spectra.[7]

Complexes of the type $[Ni\{S_2C_2(CN)_2\}(L\text{–}L)]$ where L–L = $Ph_2P(CH_2)_nPPh_2$ (n = 1, 2, 3 or 4) have been prepared and studied using the SEESR technique.[8] Their one-electron reduction products were characterised as square-planar nickel(I) species exhibiting hyperfine coupling to two equivalent ^{31}P ($I = \frac{1}{2}$) nuclei. Any oxidation processes which were observed were generally complex and irreversible.[8]

For the complexes $[M(S_2C_2Ph_2)(dppe)]$ (M = Ni, Pd or Pt), reversible one-electron oxidation processes were identified as being ligand-based, producing metal-stabilised co-ordinated dithioketyl cationic ligands.[7]

In these and related studies of mixed-ligand complexes involving bidentate phosphine and sulfur ligands, attention was primarily focused on the effects of variations in the nature of the bidentate sulfur ligand on the redox chemistry of the complexes and the nature of the products formed. In most cases the bidentate phosphine ligand used was bis(diphenylphosphino)ethane.[7–9] Variations in the phosphine ligands were restricted to the type $Ph_2P(CH_2)_nPPh_2$ which contain the saturated interphosphorus linkage $(CH_2)_n$ (n = 1, 2 or 3).[8] Previous studies have shown that bidentate ligands containing unsaturated linkages such as C_2H_2 or the *o*-phenylene group C_6H_4 are able to stabilise higher oxidation states of Ni.[10,11] It is possible that the presence of the unsaturated linkage provides an additional route for delocalisation of electrons which assists in stabilising unusual oxidation states of the metal. In order to investigate this effect further, we have prepared a number of complexes containing bidentate phosphine ligands which contain these unsaturated linkages.[12] Further, it is known that the other substituents on the phosphorus atom have a significant effect on the electron donor properties of the ligand,[13] and these may also determine the type of redox behaviour which the complexes can undergo. We have investigated this also by preparing complexes in which the terminal substituents at the phosphorus atoms are varied. The mixed ligand complexes involving bidentate phosphine ligands are **1**–**11**. In addition to these, the complexes **12**–**17** involving the non-chelating *trans* isomers of ligands with the C_2H_2 linkage were prepared, and the electrochemical and magnetic resonance studies indicated that these have the dinuclear structures shown.

We report here the preparation, characterisation and electrochemical redox processes for the nickel(II) complexes **1**–**17**.

---

† *Non-SI unit employed:* G = 10^{-4} T.

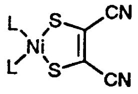

	L
1	$PMePh_2$
2	PBu^nPh_2

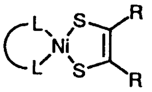

	L—L	R
3	*cis*-$Ph_2PCH{=}CHPPh_2$	CN
4	$C_6H_4(PMePh)(PPh_2)$-1, 2	CN
5	$C_6H_4(PMePh)_2$-1, 2	CN
6	$C_6H_4(PBu^nPh)(PPh_2)$-1, 2	CN
7	*cis*-$Ph_2PCH{=}CHPPh_2$	Ph
8	$C_6H_4(PMePh)(PPh_2)$-1, 2	Ph
9	$C_6H_4(PMePh)_2$-1, 2	Ph
10	$C_6H_4(PBu^nPh)(PPh_2)$-1, 2	Ph
11	$C_6H_4(PMe_2)(PPh_2)$-1, 2	Ph

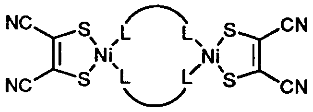

	L—L
12	*trans*-$Ph_2PCH{=}CHPPh_2$
13	*trans*-$PhMePCH{=}CHPMePh$

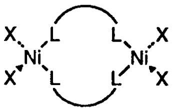

L—L *trans*-$Ph_2PCH{=}CHPPh_2$

	X
14	Cl
15	Br
16	I
17	SCN

Experimental

Electrochemistry.—The cyclic voltammograms were recorded on a Hewlett Packard 7046A XY recorder and were produced with a Princeton Applied Research (PAR) M175 Universal Programmer. The potentiostat used for the cyclic voltammetry experiments was a PAR M173. The potentiostat used for *in situ* electrolysis in the ESR tubes was a PAR M363.

The cell used for the cyclic voltammetry experiments had a three-electrode arrangement. The working electrode was a platinum disc of area *ca.* 0.3 cm^2. The counter electrode was a coil of platinum wire. The reference electrode was a platinum wire. The electrolysis solutions were approximately 0.1 mol dm^{-3} solutions of tetrabutylammonium perchlorate in CH_2Cl_2 with the sample solutions being approximately 10^{-3} mol dm^{-3}. The solution was deoxygenated by bubbling oxygen-free nitrogen through the solution, and the experiments were conducted in an atmosphere of oxygen-free nitrogen. Cyclic voltammograms of the tetrabutylammonium perchlorate solutions were recorded immediately prior to recording the cyclic voltammograms of the sample solutions, to establish the baselines for the latter. Cyclic voltammograms of the sample solutions were recorded at 50, 100, 200 and 500 mV s^{-1}. Ferrocene was then added as an internal reference and the cyclic voltammograms were recorded again.

The cyclic voltammetry parameters reported are the scan rate, the half-wave potential $E_{p/2}$, being the average of the potentials of the extrema of the anodic and cathodic wave heights, the peak to peak separation ΔE_{pp}, being the difference of those potentials, and the current ratio i_{pa}/i_{pc}, being the ratio of extrema of anodic wave height and cathodic wave height. For values of ΔE_{pp} greatly in excess of $59/n$ mV, a quasireversible or irreversible electrode process was assigned. The $E_{p/2}$ value provides an estimate of the formal potential of the redox process. All potentials were internally referenced to the Ag–AgCl couple using the potential for the one-electron oxidation of ferrocene (0.46 V *vs.* Ag–AgCl).[6]

The cell used for the *in situ* ESR experiments was similar to that described previously,[6] and consisted of a three-electrode arrangement. The working electrode was a platinum wire, and the reference electrode was a platinum wire which was sheathed in glass to within 2 mm of the working electrode. That part of the cell which extended into the ESR cavity was flattened to minimise dielectric loss. The sample solutions for these experiments were prepared and transferred to the cell using Schlenk techniques, the concentration of the degassed solutions being approximately 0.1 mol dm^{-3} in tetrabutylammonium perchlorate, and approximately 10^{-3} mol dm^{-3} in the metal complex. The *in situ* cell was sealed under nitrogen with Teflon tape, placed in the ESR cavity, and then electrolysed at a potential obtained from the cyclic voltammetry experiments. ESR spectra of the electogenerated products were then recorded.

Electron Spin Resonance Spectroscopy.—X-Band ESR spectra were recorded with a Varian E4 spectrometer. Spectra were measured and simulated as previously reported.[6]

Syntheses.—The following compounds were used in the synthesis of the ligands or of the nickel complexes, and were prepared and characterised by methods which are described elsewhere: methyldiphenylphosphine, $PMePh_2$,[12,14] *n*-butyldiphenylphosphine, PBu^nPh_2,[15] *cis*-ethenylenebis(diphenylphosphine), *cis*-$Ph_2PCH{=}CHPPh_2$,[16–18] methylphenylphosphine, PHMePh,[14,19] *rac*- and *meso*-1,2-phenylenebis(methylphenylphosphine), *rac*- and *meso*-$C_6H_4(PMePh)_2$-1,2,[14] C_6H_4-$(PMePh)(PPh_2)$-1,2,[12] $C_6H_4(PBu^nPh)(PPh_2)$-1,2,[12] C_6H_4-$(PMe_2)(PPh_2)$-1,2,[12] *trans*-$Ph_2PCH{=}CHPPh_2$ and *rac*- and *meso*-*trans*-$PhMePCH{=}CHPMePh$.[12]

The compounds [*cis*-1,2-dicyanoethene-1,2-dithiolato(2 –)-*S*,*S*′]bis(triphenylphosphine)nickel, $[Ni\{S_2C_2(CN)_2\}(PPh_3)_2]$ and bis[1,2-diphenylethene-1,2-dithiolato(1 –)-*S*,*S*′]nickel $[Ni(S_2C_2Ph_2)_2]$ were prepared by previously reported methods.[20,21]

The complexes $[Ni\{S_2C_2(CN)_2\}L_2]$ **1**, **2** were prepared by reaction of an excess of L with $[Ni\{S_2C_2(CN)_2\}(PPh_3)_2]$ (mole ratio *ca.* 3 : 1) in acetone. The complexes $[Ni\{S_2C_2(CN)_2\}$(L–L)] **3–6**, **12**, **13** were prepared by reaction of approximately equimolar amounts of L–L with $[Ni\{S_2C_2(CN)_2\}(PPh_3)_2]$ in acetone. A representative synthesis is as follows.

[cis-1,2-*Dicyanoethene*-1,2-*dithiolato*(2 –)-S,S′]*bis*(*methyldiphenylphosphine*)*nickel*, $[Ni\{S_2C_2(CN)_2\}(PMePh_2)_2]$ **1**. This compound was obtained from the reaction of $PMePh_2$ (1.48 g, 7.37 mmol) and $[Ni\{S_2C_2(CN)_2\}(PPh_3)_2]$ (1.83 g, 2.52 mmol) in an atmosphere of dry oxygen-free nitrogen in degassed acetone (50 cm^3) with stirring for 30 min. The dark red solution was filtered. The solvent was reduced in volume to precipitate a solid which was recrystallised from CH_2Cl_2–ethanol and twice recrystallised from CH_2Cl_2–diethyl ether, and dried *in vacuo* to yield red *crystals* of $[Ni\{S_2C_2(CN)_2\}(PMePh_2)_2]$ **1** (0.80 g, 53%).

The complexes $[Ni(S_2C_2Ph_2)$(L–L)] **7–11** were prepared from L–L and $[Ni(S_2C_2Ph_2)_2]$ in a manner similar to that reported for $[Ni(S_2C_2Ph_2)($*cis*-$Ph_2PCH{=}CHPPh_2)]$.[22]

The colours, yields, melting points, analytical data, and ^{31}P NMR parameters for the new complexes **1–13** are given in Tables 1 and 2.

Dihalogeno[trans-*ethenylenebis*(*diphenylphosphine*-P,P′)]-*nickel*, $[\{NiX_2($*trans*-$Ph_2PCH{=}CHPPh_2)\}_n]$ (X = Cl, Br, I or SCN), **14–17**. These compounds were prepared by a previously reported method[27] and were characterised by their melting

Table 1 Synthesis and analytical data for the diphosphine nickel(II) complexes

Compound	Colour	Yield (%)	M.p./°C	Analyses[a] (%) C	H
$[Ni\{S_2C_2(CN)_2\}(PMePh_2)_2]$ **1**	Red	53	208–210	60.1 (60.1)	4.4 (4.7)
$[Ni\{S_2C_2(CN)_2\}(PBu^nPh_2)_2]$ **2**	Green	59	170–172	63.3 (63.3)	5.6 (5.9)
$[Ni\{S_2C_2(CN)_2\}($*cis*-$Ph_2PCH{=}CHPPh_2)]$ **3**	Red	48	170–172	60.8 (60.5)	3.7 (4.1)
$[Ni\{S_2C_2(CN)_2\}\{C_6H_4(PMePh)(PPh_2)$-1,2$\}]$ **4**	Brown	22	141–142	59.2 (59.7)	3.8 (4.6)
rac-, *meso*-$[Ni\{S_2C_2(CN)_2\}\{C_6H_4(PMePh)_2$-1,2$\}]$ **5**	Orange	76	297–300	55.7 (55.3)	3.9 (4.5)
$[Ni\{S_2C_2(CN)_2\}\{C_6H_4(PBu^nPh)(PPh_2)$-1,2$\}]$ **6**	Red	75	210[b]	60.9 (61.5)	4.5 (4.9)
$[Ni(S_2C_2Ph_2)($*cis*-$Ph_2PCH{=}CHPPh_2)]$ **7**	Light green	70	162[b]	67.9 (68.9)	4.6 (5.0)
$[Ni(S_2C_2Ph_2)\{C_6H_4(PMePh)(PPh_2)$-1,2$\}]$ **8**	Light green	25	157–158	67.7 (68.3)	4.7 (5.1)
rac-, *meso*-$[Ni(S_2C_2Ph_2)\{C_6H_4(PMePh)_2$-1,2$\}]$ **9**	Grey	52	158[b]	65.7 (65.5)	4.9 (5.5)
$[Ni(S_2C_2Ph_2)\{C_6H_4(PBu^nPh)(PPh_2)$-1,2$\}]$ **10**	Light green	19	294–296	68.7 (69.3)	5.3 (5.9)
$[Ni(S_2C_2Ph_2)\{C_6H_4(PMe_2)(PPh_2)$-1,2$\}]$ **11**	Light green	26	167–168	65.4 (65.4)	5.0 (5.6)
$[\{Ni[S_2C_2(CN)_2]($*trans*-$Ph_2PCH{=}CHPPh_2)\}_2]$ **12**	Green	51	255–262	60.4 (60.5)	3.7 (3.9)
$[\{Ni[S_2C_2(CN)_2]($*trans*-$PhMePCH{=}CHPMePh)\}_2]$ **13**	Brown	62	189–191	51.3 (51.0)	3.9 (4.5)

[a] Required values are given in parentheses. [b] With decomposition.

Table 2 ^{31}P NMR parameters for the diphosphine nickel(II) complexes

Compound	δ_C[a]	$^3J(PP)$/Hz	δ_L[b]	Δ_C/ppm[c]	Δ_B/ppm[d]	Δ_R/ppm[e]
$[Ni\{S_2C_2(CN)_2\}(PPh_3)_2]$	26.6		−6.0	32.6	32.6	—
1	10.3		−26.0	36.3	36.3	—
2	17.6		−17.1	34.7	34.7	—
$[Ni\{S_2C_2(CN)_2\}(Ph_2PCH_2CH_2PPh_2)]$	59.9		−12.5	72.4	32.6	39.8
3	68.6		−22.8	91.4	32.6	58.8
4	46.7 (PMePh)	53.7	−31.3 (PMePh)	78.0	36.3[f]	41.7[f]
	60.0 (PPh_2)		−13.3 (PPh_2)	73.3	32.6[f]	40.7[f]
5	49.3, 48.3[g]		−35.5, −36.1[g]	84.6[h]	36.3	48.3
6	57.6 (PBu^nPh)	52.9	−27.2 (PBu^nPh)	84.8	34.7[f]	50.1[f]
	60.8 (PPh_2)		−13.4 (PPh_2)	74.2	32.6[f]	41.6[f]
7	63.8		−22.8	86.6	32.6	54.0
8	43.6 (PMePh)	47.6	−31.3 (PMePh)	74.9	36.3[f]	38.6[f]
	57.9 (PPh_2)		−13.3 (PPh_2)	71.2	32.6[f]	38.6[f]
9	46.5, 45.1[g]		−35.5, −36.1[g]	81.6[h]	36.6	45.0
10	54.0 (PBu^nPh)	47.6	−27.2 (PBu^nPh)	81.2	34.7[f]	46.5[f]
	58.7 (PPh_2)		−13.4 (PPh_2)	72.1	32.6[f]	39.5[f]
12	24.3		−7.7	32.0	32.6	−0.6

[a] δ_C = ^{31}P chemical shift for the complexed ligand. [b] δ_L = ^{31}P chemical shift for the uncomplexed ligand; this work or refs 18, 23–26. [c] $\Delta_C = \delta_C - \delta_L$. [d] $\Delta_B = \Delta_C$ of the corresponding bis(tertiary phosphine) nickel(II) complex. [e] $\Delta_R = \Delta_C - \Delta_B$ (see text). [f] Δ_B and Δ_R values are estimates only, using the values of Δ_B for $[Ni\{S_2C_2(CN)_2\}(PPhR_2)_2]$. [g] Two diastereoisomers. [h] Average value.

points [X = Cl, m.p. 190–195 °C (lit.[27], 175–180 °C) **14**; X = Br, m.p. 220–225 °C (lit.[27], 210 °C) **15**; X = I, m.p. 210–220 °C (lit.[27], 202–208 °C) **16**; X = SCN, m.p. 195–200 °C (lit.[27], 185–193 °C) **17**].

Results and Discussion

*Phosphorus-*31 *NMR Spectroscopy of the Nickel*(II) *Compounds.*—In order to identify the new diphosphinonickel(II) complexes and to ascertain their structure, ^{31}P NMR spectra were recorded. The ^{31}P NMR data are given in Table 2 and show three distinct groups of complexes, (*i*) bis(tertiary phosphine) complexes **1** and **2**; (*ii*) ditertiary phosphine chelate complexes **3**–**11** and (*iii*) ditertiary phosphine Ni–Ni dimers **12**–**17**. These groups are characterised as shown in the following.

The ^{31}P NMR chemical shifts, δ_C for phosphorus nuclei in diphosphine nickel(II) complexes are given in Table 2 together with δ_L, the chemical shifts of the unco-ordinated tertiary phosphine or ditertiary phosphine. The parameters Δ_C and Δ_R are also given, where $\Delta_C = \delta_C - \delta_L$ and is the co-ordination chemical shift. The Δ_C parameter measures a net change in the chemical shift upon complexation of a ligand. The Δ_R is given by $\Delta_R = \Delta_C - \Delta_B$ and is the ring contribution[28,29] to the chemical shift. The Δ_R parameter measures the difference between the co-ordination chemical shift of $[Ni\{S_2C_2(CN)_2\}(R^1R^2PR^3PR^1R^2)]$, Δ_C and the co-ordination chemical shift of $[Ni\{S_2C_2(CN)_2\}(PR^1R^2Ph)_2]$, Δ_B. The Δ_R value measures the influence of the interphosphorus linkage R^3 upon the chemical shift. Thus Δ_C is a characteristic of the net effect of complexation upon the ^{31}P NMR chemical shift, whereas Δ_R is a characteristic of the effect of the interphosphorus linkage.

First, considering complexation effects, inspection of Table 2 reveals that the Δ_C values lie in two ranges, 32.0–36.3 ppm and 71.2–91.4 ppm. The former range is characteristic of the decrease in shielding on complexation to form bis(tertiary phosphine) complexes. The latter range is characteristic[28] of the decrease in shielding about the phosphorus nuclei, produced by complexation to form a five-membered chelate.

Secondly, considering ring contribution effects, the Δ_R value for the *trans*-linkage of compound **12**, $[\{Ni[S_2C_2(CN)_2]($*trans*-$Ph_2PCH{=}CHPPh_2)\}_2]$, is small and negative in contrast to the large positive[28] Δ_R values for the five-membered ring chelate complexes. The anomalous result for compound **12** can be explained in terms of a model of a ten-membered ring as depicted in Fig. 1(*a*). This model, in which the complex has C_{2h} symmetry, is consistent with the ^{31}P NMR spectrum, which exhibits one peak due to four chemically equivalent phosphorus nuclei. The assignment of a Ni–Ni dimer model allows the complex to be considered as consisting of two identical nickel(II) centres, each co-ordinated by a diphosphino ligand with a seven-membered linkage to produce, with the nickel(II) centre, a ten-membered chelate, as depicted in Fig. 1(*b*). The small and

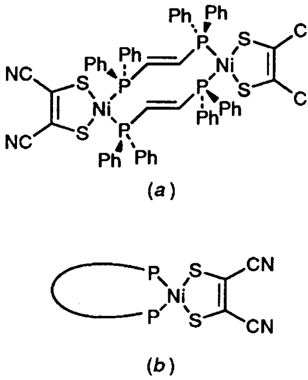

(a)

(b)

Fig. 1 (a) A dimeric structure for compound **12**, with C_{2h} symmetry and (b) a conceptualisation of the dimer as a monomer with a large chelate

negative Δ_R value of compound **12** may thus be considered as the ring contribution for this pseudo-ten-membered ring, and this is similar in magnitude to the ring contributions observed for four- and six-membered chelates.[28]

Electrochemical and ESR Investigation.—The maleonitriledithiolate complexes **1–6**, **12** *and* **13**. (a) *Reduction processes.* The compounds **1–6** each showed a quasi-reversible reduction in CH_2Cl_2; the cyclic voltammetry parameters are listed in Table 3. Controlled potential electrolysis in the *in situ* ESR cell resulted in spectra similar to those reported previously for the one-electron reduction products of $[Ni\{S_2C_2(CN)_2\}(PPh_3)_2]$ or $[Ni\{S_2C_2(CN)_2\}(dppe)]$,[8] showing hyperfine coupling to two equivalent ^{31}P, and anisotropic *g*-tensor components with near axial symmetry. The *g* values are characteristic of d^9 nickel(I) species with an unpaired electron localised mainly in the nickel $d_{x^2-y^2}$ orbital.[6,8] The ESR parameters are given in Table 4. This indicates that the reduction process involved is given by equation (1). For compound **5**, although two diastereoisomers

$$[Ni\{S_2C_2(CN)_2\}(L\text{–}L)] + e^- \rightleftharpoons [Ni\{S_2C_2(CN)_2\}(L\text{–}L)]^- \quad (1)$$

are present, only one reduction wave was evident in the cyclic voltammogram. Although compounds **4** and **6** contain unsymmetrical ditertiary phosphines, the ESR spectra of their one-electron reduction products exhibited equal coupling to the two ^{31}P nuclei.

The compounds **12** and **13** may be di- or multi-nuclear,[27] because their ditertiary phosphine ligands are non-chelating. The compound **12** shows a ^{31}P NMR spectrum characteristic of a dinuclear species as indicated above. The cyclic voltammetry and ESR data provide further evidence in support of a dinuclear structure for these complexes. They each exhibit two successive quasi-reversible reductions in CH_2Cl_2. The cyclic voltammetry parameters are given in Table 3. Controlled potential electrolysis at a potential midway between the two half-wave potentials in the *in situ* ESR cell produced spectra similar to those observed for the mononuclear complexes. This establishes that the first reduction process involves transfer of one electron which is localised on one nickel atom. The fact that the two successive one-electron reduction waves are of similar height indicates that the second step also involves a one-electron reduction, presumably centred on a second Ni atom in the complex. These observations therefore support the proposed dinuclear structure,[30,31] which consists of a $Ni\{S_2C_2(CN)_2\}$ moiety and a diphosphine moiety with a large linkage as depicted in Fig. 1(b). The difference between the $E_{p/2}$ values of the successive reduction processes for each complex are similar, being 0.23 and 0.25 V respectively.

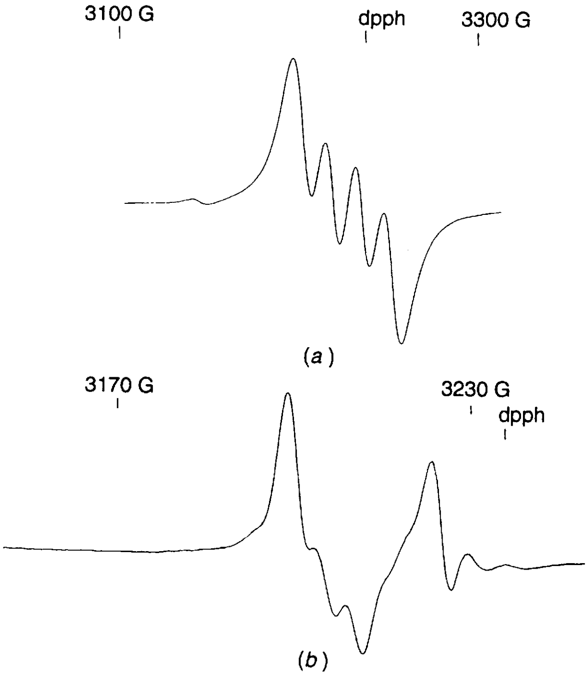

(a)

(b)

Fig. 2 ESR spectra of the electrogenerated oxidation product of $[Ni\{S_2C_2(CN)_2\}\{C_6H_4(PMePh)(PPh_2)\text{-}1,2\}]$ **4** in CH_2Cl_2. (a) Solution spectrum at *ca.* 298 K and (b) frozen solution spectrum at *ca.* 90 K (dpph = diphenylpicrylhydrazyl)

(b) *The oxidation processes.* The compound **13** exhibits two reversible oxidation processes, whose cyclic voltammetric waves have current peak heights which are similar in magnitude to those of the waves assigned to the successive one-electron reductions. The two oxidation processes are thus assigned as two one-electron oxidations. The cyclic voltammetric parameters are given in Table 3. The difference between the first and second oxidation $E_{p/2}$ values is 0.19 ±0.03 V and this can be compared with the value 0.25 ± 0.03 V which is the difference between the first and second reversible reduction $E_{p/2}$ values. That these differences are similar in magnitude indicates that similar changes occur to the complex following both electron transfers. The ability of compound **13** to exhibit two reversible oxidation processes whereas compound **12** does not exhibit any such processes may be attributed to the σ-donor effect of the methyl substituents on the phosphorus atoms; previous studies have shown that methyl substituted ditertiary phosphine ligands such as $C_6H_4(PMe_2)_2\text{-}1,2$ can stabilise the higher oxidation states of nickel.[10] No ESR spectrum was exhibited by the solution nor the frozen solution of the product of controlled potential electrolysis of **13** at a potential midway between the $E_{p/2}$ values for the two oxidation processes. Hence the identity of the oxidation products was not determined.

The compounds **3–5** exhibit irreversible oxidation processes whose E_{pa} values are in the range 1.21 ± 0.04 to 1.25 ± 0.04 V at a scan rate of 100 mV s^{-1}. Controlled potential electrolysis of **3** and **5** in the *in situ* ESR cell produced solution and frozen solution spectra which were assignable to the $[Ni\{S_2C_2(CN)_2\}_2]^-$ ion, which has a characteristic ESR spectrum.[32] Compound **4**, however, exhibited solution and frozen solution spectra as shown in Fig. 2. The solution spectrum exhibits a four-line pattern with the parameters given in Table 4. The four-line pattern is indicative of coupling to two inequivalent ^{31}P nuclei. The *g* value is close to the g_e value and is not characteristic of the *g* values observed for d^7 nickel(III) complexes with metal-based unpaired electrons.[33] The *g* value and hyperfine coupling constants are however characteristic of the ESR parameters obtained for PR_3^+ radicals (R = Et and Bu^n).[34] In the present case, the ESR spectra are consistent with the presence of a nickel(II)-stabilised co-ordinated radical cation, such that it is

Table 3 Cyclic voltammetry parameters for the redox processes of the maleonitriledithiolate complexes[a]

Complex	Ring size	$E_{p/2}$/V	ΔE_{pp}/V[b]	i_{pa}/i_{pc}[b]	ΔE_{pp}/V[c]	i_{pa}/i_{pc}[c]
$[Ni\{S_2C_2(CN)_2\}(PPh_3)_2]$	—	−0.74	0.09	—	—	—
1	—	−0.93	0.15	0.1	0.08	0.05
2	—	−0.82	0.15	0.1	0.05	0.05
$[Ni\{S_2C_2(CN)_2\}(Ph_2PCH_2PPh_2)]$	4	−1.08	0.06	—	—	—
$[Ni\{S_2C_2(CN)_2\}(Ph_2PCH_2CH_2PPh_2)]$	5	−1.20	0.07	—	—	—
3	5	−1.07	0.10	0.4	0.08	0.40
4	5	−1.16	0.13	0.1	0.13	0.10
5	5	−1.23	0.24	0.5	0.15	0.90
6	5	−1.22	0.13	0.1	0.08	0.05
$[Ni\{S_2C_2(CN)_2\}\{Ph_2P(CH_2)_4PPh_2\}]$[d]	7	−1.06	0.22	—	—	—
12	10	−0.55	0.05	0.4	0.03	0.30
	10	−0.78	0.13	0.30	0.09	0.30
13	10	−0.70	0.10	0.20	0.10	0.10
	10	−0.95	0.18	0.30	0.10	0.30
	10	0.28	0.05	0.30	0.05	0.80
	10	0.47	0.08	0.30	0.45	0.50

[a] The data are for CH_2Cl_2 solutions of the compounds at *ca.* 298 K. [b] Scan rate 200 mV s^{-1}. [c] Scan rate 50 mV s^{-1}. [d] Ref. 8.

Table 4 ESR parameters for the electrogenerated maleonitriledithiolate species[a]

Assigned ESR active species	Ring size[b]	g_{iso}[c]	g_1[d]	g_2[d]	g_3[d]	A_{iso}[e]	A_1[f]	A_2[f]	A_3[f]
$[Ni\{S_2C_2(CN)_2\}(PPh_3)_2]^-$[g]	—	2.082	2.193	2.066	2.066	91	84	95	95
$\mathbf{1}^-$	—	2.062	2.192	2.063	2.060	102	92	100	90
$\mathbf{2}^-$[g]	—	2.087	2.187	2.050	2.050	98	94	98	98
$[Ni\{S_2C_2(CN)_2\}(Ph_2PCH_2PPh_2)]^-$[g]	4	2.081	2.187	2.049	2.049	97	105	98	98
$[Ni\{S_2C_2(CN)_2\}(Ph_2PCH_2CH_2PPh_2)]^-$[g]	5	2.079	2.161	2.043	2.036	104	92	103	112
$\mathbf{3}^-$	5	2.079	2.148	2.050	2.037	104	100	105	115
$\mathbf{4}^-$	5	2.077	2.131	2.041	2.028	105	100	103	115
$\mathbf{5}^-$	5	2.072	2.140	2.042	2.037	107	90	105	118
$\mathbf{6}^-$	5	2.079	2.140	2.040	2.037	104	110	88	130
$[Ni\{S_2C_2(CN)_2\}\{Ph_2P(CH_2)_4PPh_2\}]^-$[g]	7	2.094	2.177	2.045	2.045	99	93	103	103
$\mathbf{12}^-$	10	2.085	2.175	2.053	2.046	90	88	90	97
$\mathbf{13}^-$	10	2.072	2.173	2.048	2.044	97	70	100	100
$\mathbf{4}^+$	5	2.079[h]	*i*	*i*	*i*	16, 32[h]	*i*	*i*	*i*

[a] In CH_2Cl_2 solution. Isotropic and anisotropic parameters were obtained at *ca.* 298 and *ca.* 90 K respectively. [b] See text. [c] Isotropic *g* value. [d] Anisotropic *g* values. [e] Isotropic hyperfine coupling constant (10^{-4} cm^{-1}). [f] Anisotropic hyperfine coupling constant (10^{-4} cm^{-1}). [g] Ref. 8. [h] Spectrum shows hyperfine coupling to two inequivalent ^{31}P, Fig. 2(*a*). [i] Spectrum too complex to allow unambiguous analysis, Fig. 2(*b*).

the co-ordinated ditertiary phosphine ligand which has undergone an irreversible one-electron oxidation.[7]

(*c*) *Ligand effects on the electrochemical and EPR parameters.* The effects of variations in the nature of the phosphine ligand on the electronic properties of the complexes concerned can be investigated *via* their reduction potentials and EPR parameters. The reduction potential gives an indication of the ease with which an electron can be added to the complex, and so is related to the energy of the lowest unoccupied molecular orbital (LUMO) in the oxidised form of the complex. The EPR parameters give information about the distribution of the unpaired electron in the highest occupied molecular orbital (HOMO) of the reduced form. In the present study the phosphine ligand was varied, and these variations can be discussed in terms of a number of parameters, as described below.

(*i*) *The ring size.* This is defined as the number of atoms in the chelate ring formed by the phosphine ligand. The compounds **1** and **2** have no linkage between the co-ordinating phosphorus atoms, and so their ring size is not defined. The compounds **3**–**6** have ring sizes of five while compounds **12** and **13** may be considered to have ring sizes of ten. The reduction potentials $E_{p/2}$ in Table 3 show a clear dependence on ring size, the values for the five-membered rings being more negative than those for the ten-membered ring or non-chelate phosphine ligand complexes. This behaviour is similar to that of the co-ordination chemical shifts of these compounds as discussed above. Similar behaviour is also seen in the EPR parameters in Table 4, and is most clearly evident in the values of the *g*-tensor component g_1. The difference between this and the free electron value g_e = 2.0023 is a measure of the degree of localisation of the unpaired electron on the Ni atom. This is due to a larger degree of spin–orbit coupling at the nickel atom, and contrasts with the case where an unpaired electron is largely ligand based.[7] The one-electron reduction products of **1** and **2** exhibit the greatest *g* value shift and this is consistent with the absence of a ring. Hence the unpaired electron is more localised at the nickel centre. The one-electron reduction products of **3**–**6** show a lesser *g* value shift as would be expected, since in these cases delocalisation over unsaturated linkages is possible (see below). The *g* values of the one-electron reduction products of **12** and **13** show that, although a large ring system is available for delocalisation, the unpaired electron is metal-based to an extent intermediate between the extremes of the one-electron reduction products of compounds **1**–**6**. The hyperfine coupling constants in Table 4 do not vary much with ring size, although the values for the complexes with a ring size of five appear to be slightly higher than the others, suggesting a slightly greater degree of delocalisation of the unpaired electron onto the phosphorus atoms in these cases. Smaller variations in the redox and EPR parameters for complexes with the same ring size are apparent, indicating that these parameters are also influenced by factors other than the ring size, as discussed below.

(*ii*) *The interphosphorus linkage.* The effect of establishing a link between the phosphorus atoms to form a chelate can be investigated by comparing the properties of the chelate complex with those of the corresponding non-chelate complex in which the linkage is replaced at each phosphorus atom by a terminal organic group. In the present study the phenyl group has been

Table 5 The effect of an interphosphorus linkage on cyclic voltammetry (200 mV s^{-1}) and ESR parameters for various $[\{Ni[S_2C_2(CN)_2](L–L)\}_n]$ complexes (n = 1 or 2)

Chelate complex (1)	Ring size	Corresponding non-chelate complex (2)	$E_{p/2}(1)$/V[a]	$E_{p/2}(2)$/V[b]	$\Delta E_{p/2}$/V[c]	$g_1(1)$[a]	$g_1(2)$[b]	Δg_1[c]
$[Ni\{S_2C_2(CN)_2\}(Ph_2PCH_2PPh_2)]$	4	$[Ni\{S_2C_2(CN)_2\}(PPh_3)_2]$	−1.08[d]	−0.74[d]	−0.34	2.187	2.193[d]	−0.006
$[Ni\{S_2C_2(CN)_2\}(Ph_2PCH_2CH_2PPh_2)]$	5	$[Ni\{S_2C_2(CN)_2\}(PPh_3)_2]$	−1.20[d]	−0.74[d]	−0.46	2.161[d]	2.193[d]	−0.032
3	5	$[Ni\{S_2C_2(CN)_2\}(PPh_3)_2]$	−1.07	−0.74[d]	−0.33	2.148	2.193[d]	−0.045
5	5	$[Ni\{S_2C_2(CN)_2\}(PMePh_2)_2]$	−1.23	−0.93	−0.30	2.140	2.192	−0.052
$[Ni\{S_2C_2(CN)_2\}\{Ph_2P(CH_2)_4PPh_2\}]$	7	$[Ni\{S_2C_2(CN)_2\}(PPh_3)_2]$	−1.06[d]	−0.74[d]	−0.32	2.177[d]	2.193[d]	−0.016
12	10	$[Ni\{S_2C_2(CN)_2\}(PPh_3)_2]$	−0.55	−0.74[d]	+0.19	2.175	2.193[d]	−0.018
13	10	$[Ni\{S_2C_2(CN)_2\}(PMePh_2)]_2$	−0.70	−0.93	+0.23	2.173	2.192	−0.019

[a] Parameter value for chelate (1) or its reduction product. [b] Paremater value for non-chelate (2) or its reduction product. [c] Difference between parameter values for corresponding chelate and non-chelate complexes (1) and (2). [d] Ref. 8.

used for this purpose. The change in the one-elecron $E_{p/2}$ values and the g_1 values for pairs of complexes related in this way are given in Table 5. This analysis is similar to that used in the calculation of the ring contribution to the ^{31}P NMR chemical shift for the same compounds (see above). The $\Delta E_{p/2}$ values in Table 5 show the change in $E_{p/2}$ brought about by the addition of a linkage between the co-ordinating phosphorus atoms. The data clearly show that, despite changes in ring size, the incorporation of a linkage results in an anodic shift of about 0.4 V in the one-electron reduction potential when the ligand is a chelate. However, when the ligand is a non-chelate, as for compounds **12** and **13**, there is a cathodic shift of about 0.2 V. The first of the two successive reductions of compounds **12** and **13** was assigned as a one-electron reduction localised at one nickel centre as discussed above, but the reduction potential may still be influenced by the presence of the second nickel centre in the dimer. This could occur *via* (*a*) an electronic interaction between the d orbitals on the two Ni atoms (by direct overlap, or *via* the connecting ligands),[35,36] or (*b*) a 'through-space' electrostatic interaction between the nickel(II) centre and the electron localised at the other nickel centre.[37] A direct interaction between the orbitals on the two nickel atoms seems unlikely in view of the large separation between the atoms, and extensive delocalisation of the unpaired electron over the ligands in the one-electron reduction product is not compatible with the ESR results. This suggests that the cathodic shift is due to a through-space electrostatic interaction.

(*iii*) *Substituent effects.* The alkyl or aryl substituents in a phosphine ligand affect the σ-donicity of the ligand, as indicated by the pK_a value of the conjugate acid.[38] Small but systematic changes in the one-electron reduction potentials in Table 3 can be attributed to changes in the substituents in the ligands. Thus, replacement of a Me group with a Bu^n group produces a change in the $E_{p/2}$ value of −0.06 ± 0.04 V (compounds **4** and **6**), and replacement of a phenyl group by a methyl changes $E_{p/2}$ by −0.09 ± 0.04 V (compounds **4** and **5**, **12** and **13** and **1** and $[Ni\{S_2C_2(CN)_2\}(PPh_3)_2]$. This indicates an increase in the σ-donor power of the ligand as the phenyl groups are replaced by the more strongly σ-donating methyl groups. A similar result is observed for the A_{iso} values for the one-electron reduction products which increase by (8 ± 3) × 10^{-4} cm^{-1} for each phenyl group substituted by a methyl group. This suggests an increase in s character of the phosphorus donor orbital.[39]

Compounds $[Ni(S_2C_2Ph_2)(L–L)]$ **7**–**11**.—The cyclic voltammetry parameters for compounds **7**–**11** as given in Table 6 show that these undergo both a reduction and an oxidation process. Except for compound **8**, they also exhibit a second oxidation process. The reduction process and the first oxidation process are quasi-reversible.

The solution ESR spectra obtained in the *in situ* ESR cell after controlled potential electrolysis of compounds **7**–**10** at a potential in excess of the $E_{p/2}$ for the oxidation process all showed triplet patterns due to coupling with two equivalent ^{31}P. The ESR parameters are listed in Table 7. These spectra indicate that the one-electron oxidation products were nickel(II)-stabilised ligand radical cations, as for similar previously reported compounds.[7]

While oxidation products of compounds **7** and **10** exhibited frozen-solution ESR spectra (Table 7) which showed no ^{31}P coupling, the oxidation product of compound **8** at *ca.* 90 K showed only a very weak spectrum while that of **9** exhibited no frozen-solution ESR spectrum at all. When the frozen solution was allowed to warm slowly to room temperature in the latter two cases, the solution ESR spectrum which was observed prior to freezing reappeared with no loss of intensity. This result might be explained by the rapid reversible formation of an ESR inactive species, such as a dimer, as the solution is quickly frozen. Dimeric structures have been reported for mixed ligand–dithiolate complexes.[40]

The products of the *in situ* electrolysis of the compounds **7**–**10** at a potential below that of the reduction process, showed no solution or frozen solution ESR spectra. The cathodic and anodic wave heights for the reduction process and the first oxidation process are similar in magnitude, indicating that the two processes involve the transfer of the same mole equivalent of electrons (assuming that similar diffusion coefficients apply for both processes[41]). On this basis, the reduction processes for the compounds **7**–**10** are assigned as one-electron processes. The identity of the reduction products remains unknown, however, because none of them exhibited ESR spectra. This is in contrast to the situation reported previously for $[Ni(S_2C_2Ph_2)(Ph_2PCH_2CH_2PPh_2)]$.[7]

Effects of changes in the phosphine ligands on the redox potentials of the diphenylethenedithiolate complexes were noted, and these parallel some of the findings described above for the maleonitriledithiolate complexes. Thus, for example, a comparison of the $E_{p/2}$ values for the first oxidation processes for complexes **8** and **9** (Table 6) shows that the methyl substituent produces a more anodic oxidation potential than the phenyl group. Likewise, comparing complexes **8** and **10**, the *n*-butyl substituent produces a more anodic oxidation potential than the methyl substituent. These shifts in redox potential (0.12 ± 0.06 V) are similar in magnitude, but opposite in sign to those observed for the one-electron reductions of the corresponding maleonitriledithiolate complexes.

The Halogeno Complexes $[\{NiX_2(trans\text{-}Ph_2PCH{=}CHPPh_2)\}_n]$ (X = Cl, Br, I *or* SCN) **14**–**17**.—The cyclic voltammograms of CH_2Cl_2 solutions of the compounds $[\{NiX_2(trans\text{-}Ph_2PCH{=}CHPPh_2)\}_n]$ (X = Cl, Br or SCN) exhibited single irreversible cathodic processes, whereas the iodide exhibited two quasi-reversible reduction processes. The difference between the $E_{p/2}$ values for these two processes is 0.20 V, which is similar to the values obtained for the complexes $[\{Ni[S_2C_2(CN)_2](trans\text{-}PhRPCH{=}CHPRPh)\}_2]$ (R = Me or Ph, see above).

In situ controlled potential electrolysis at potentials below

Table 6 Cyclic voltammetry parameters for the redox processes of complexes **7**–**11**[a]

		Scan rate = 200 mV s^{-1}		50 mV s^{-1}	
	$E_{p/2}$/V	ΔE_{pp}/V	i_{pa}/i_{pc}	ΔE_{pp}/V	i_{pa}/i_{pc}
Reduction process					
7	−1.79	0.13	0.40	0.09	0.30
8	−1.66	0.14	0.10	0.14	0.20
9	−1.74	0.40	0.40	0.25	0.30
10	−1.73	0.10	0.30	0.09	0.30
11	−1.34	0.20	0.1	—	—
First oxidation process					
7	0.51	0.10	0.50	0.05	0.50
8	0.43	0.08	0.30	0.05	0.20
9	0.61	0.15	0.60	0.03	0.50
10	0.48	0.08	0.60	0.06	0.40
11	0.65[b]	—	—	—	—
Second oxidation process					
7	0.99	0.10	0.90	0.09	0.50
9	2.08[b]	—	—	—	—
10	0.95	0.15	0.3	0.10	0.20
11	0.84[b]	—	—	—	—

[a] The data are for CH_2Cl_2 solutions of the complexes at *ca.* 273 K. [b] E_{pa} value.

Table 7 ESR parameters for paramagnetic species electrogenerated by oxidation of CH_2Cl_2 solutions of complexes **7**–**10**[a]

Complex	g_{iso}	$10^4 A_{iso}$/cm^{-1}	g_1[b]	g_2[b]	g_3[b]
7	2.013	4.6	2.036	2.022	2.008
10	2.014	4.4	2.095	2.017	1.987
9	2.021	4.6	*c*		
8	2.014	4.6	*d*		

[a] Isotropic spectra were obtained at 273 K and frozen solution spectra were obtained at *ca.* 90 K. [b] Estimates of principal values of *g*-tensor. [c] No frozen solution spectrum exhibited. [d] Frozen solution spectrum too weak to allow analysis.

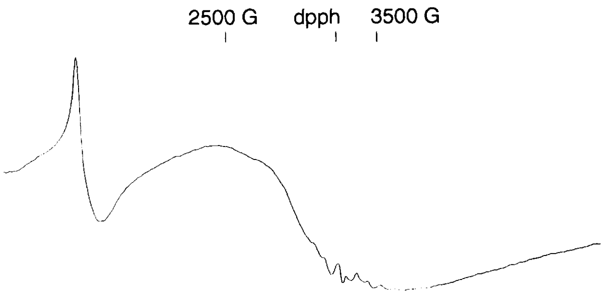

Fig. 3 Frozen-solution ESR spectrum of the product of the controlled potential reduction of [{NiI_2(*trans*-Ph_2PCH=$CHPPh_2$)}$_2$] **16**

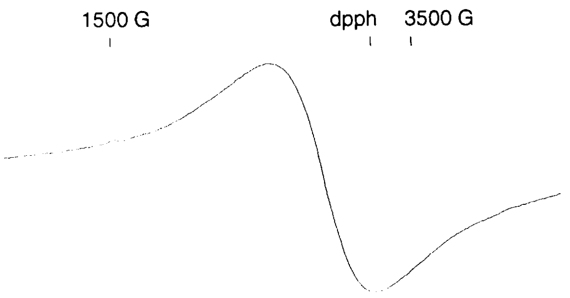

Fig. 4 Frozen-solution ESR spectrum of the product of the controlled potential reduction of [{$NiCl_2$(*trans*-Ph_2PCH=$CHPPh_2$)}$_n$] **14** in CH_2Cl_2, at *ca.* 90 K

that of the first reduction process for the iodo complex resulted in a solution which did not exhibit an ESR spectrum at room temperature. At a potential below that of the second reduction process, again, no room-temperature solution ESR spectrum was observed. However, the frozen solution did exhibit an ESR spectrum, which is shown in Fig. 3. This exhibits a broad peak with g = 2.17 (B = 2980 G) and a sharp 'half-field' peak at 1490 G. Such signals at half field are characteristic of $\Delta M_s = \pm 2$ transitions for triplet state species. The $\Delta M_s = \pm 2$ line is sharp as expected, and the broadness of the $\Delta M_s = \pm 1$ resonance near g = 2 is due to zero-field splitting. This suggests a dinuclear structure [{NiI_2(*trans*-Ph_2PCH=$CHPPh_2$)}$_2$] for the parent complex, which undergoes two successive one-electron reduction processes to produce a triplet state Ni^I–Ni^I species.

The observation of only a single irreversible reduction process for the complexes [{NiX_2(*trans*-Ph_2PCH=$CHPPh_2$)}$_n$] (X = Cl or Br), indicates that an electrochemical–chemical process occurs in these cases, probably involving loss of halide ligand following the electrochemical reduction. A broad frozen solution spectrum with g_{iso} = 2.224 and linewidth = 700 G was obtained following reduction of [{$NiCl_2$(*trans*-Ph_2PCH=$CHPPh_2$)}$_n$] as shown in Fig. 4.

Acknowledgements

We acknowledge support of this work by grants from the New Zealand University Grants Committee and the University of Auckland Research Committee.

References

1 T. M. McKinney, *Electroanal. Chem.*, 1977, **10**, 97.
2 W. J. Albery, R. G. Compton and C. C. Jones, *J. Am. Chem. Soc.*, 1984, **106**, 469.
3 C. Lamy and P. Crouigneau, *J. Electroanal. Chem. Interfacial Electrochem.*, 1983, **150**, 545.
4 J. Furhop, K. M. Kadish and D. G. Davis, *J. Am. Chem. Soc.*, 1973, **95**, 5140.
5 F. V. Lovecchio, E. S. Gore and D. H. Busch, *J. Am. Chem. Soc.*, 1973, **96**, 3109.
6 G. A. Bowmaker, P. D. W. Boyd, G. K. Campbell, J. M. Hope and R. L. Martin, *Inorg. Chem.*, 1982, **21**, 1152.
7 G. A. Bowmaker, P. D. W. Boyd and G. K. Campbell, *Inorg. Chem.*, 1983, **22**, 1208.
8 G. A. Bowmaker, P. D. W. Boyd and G. K. Campbell, *Inorg. Chem.*, 1982, **21**, 2403.
9 G. A. Bowmaker, P. D. W. Boyd, M. Zvagulis, K. J. Cavell and A. F. Masters, *Inorg. Chem.*, 1985, **24**, 401.
10 L. F. Warren and M. A. Bennett, *Inorg. Chem.*, 1976, **15**, 3126.
11 M. A. Bennett and J. D. Wild, *J. Chem. Soc. A*, 1971, 536.
12 G. A. Bowmaker and J. P. Williams, *Aust. J. Chem.*, submitted for publication.

13 S. J. Higgins, W. Levason and D. J. Wilkes, *Inorg. Chim. Acta*, 1984, **84**, 1.
14 N. K. Roberts and S. B. Wild, *J. Am. Chem. Soc.*, 1979, **101**, 6254.
15 G. M. Kosolapoff and L. Maier, *Organic Phosphorus Compounds*, Wiley Interscience, New York, 2nd edn, 1972, vol. 1, ch. 1, p. 58.
16 A. M. Aguiar and D. Daigle, *J. Am. Chem. Soc.*, 1964, **86**, 2299.
17 K. K. Chow, W. Levason and C. A. McAuliffe, *J. Chem. Soc., Dalton Trans.*, 1976, 1429.
18 R. A. Kolodny, T. L. Morris and R. C. Taylor, *J. Chem. Soc., Dalton Trans.*, 1973, 328.
19 J. Albrand, G. Gagnaire and J. Robert, *Bull. Chim. Soc. Fr.*, 1968, 479.
20 A. Davison, N. Edelstein, R. H. Holm and A. H. Maki, *Inorg. Chem.*, 1964, **3**, 814.
21 G. N. Schrauzer and V. P. Mayweg, *J. Am. Chem. Soc.*, 1965, **87**, 1483.
22 V. P. Mayweg and G. N. Schrauzer, *J. Chem. Soc., Chem. Commun.*, 1966, 640.
23 S. O. Grim, D. A. Wheatland and W. McFarlane, *J. Am. Chem. Soc.*, 1967, **89**, 5573.
24 S. O. Grim, W. McFarlane and E. F. Davidoff, *J. Org. Chem.*, 1967, **32**, 781.
25 R. C. Taylor, R. L. Keiter and L. W. Cary, *Inorg. Chem.*, 1974, **13**, 1928.
26 I. J. Colquhoun and W. McFarlane, *J. Chem. Soc., Dalton Trans.*, 1982, 1915.
27 K. K. Chow, W. Levason and C. A. McAuliffe, *Inorg. Chim. Acta*, 1973, **7**, 589.
28 P. E. Garrou, *Inorg. Chem.*, 1975, **14**, 1435.
29 P. E. Garrou, *Chem. Rev.*, 1981, **81**, 229.
30 R. R. Gagne, C. A. Koval, T. J. Smith and M. C. Gimolino, *J. Am. Chem. Soc.*, 1979, **101**, 4571.
31 D. S. Polcyn and I. Shain, *Anal. Chem.*, 1966, **38**, 370.
32 A. Davison, N. Edelstein, R. H. Holm and A. H. Maki, *J. Am. Chem. Soc.*, 1963, **85**, 2029.
33 C. N. Sethulakshmi, S. Subramainan, M. A. Bennett and P. T. Manoharan, *Inorg. Chem.*, 1979, **18**, 2520.
34 A. Begum, A. R. Lyons and M. C. R. Symons, *J. Chem. Soc. A*, 1971, 2290.
35 R. C. Long and D. N. Hendrickson, *J. Am. Chem. Soc.*, 1983, **105**, 1513.
36 A. J. Bard, *Pure Appl. Chem.*, 1971, **25**, 279.
37 W. H. Morrison Jr., E. Y. Ho and D. N. Hendrickson, *Inorg. Chem.*, 1975, **14**, 500.
38 M. N. Golovin, M. M. Rahman, J. E. Belmonte and W. P. Giering, *Organometallics*, 1985, **4**, 1981.
39 B. B. Wayland, M. E. Abd-Elmageed and L. F. Mehne, *Inorg. Chem.*, 1975, **14**, 1456.
40 R. P. Burns and C. A. McAuliffe, *Adv. Inorg. Chem. Radiochem.*, 1979, **22**, 303.
41 A. J. Bard and L. R. Faulkner, *Electrochemical Methods*, Wiley, 1970.

Received 25*th May* 1993; *Paper* 3/02979D